Phase transitions in solid C_{70}: Supercooling, metastable phases, and impurity effect

A. R. McGhie
Laboratory for Research on the Structure of Matter, University of Pennsylvania, Philadelphia, Pennsylvania 19104

J. E. Fischer
Department of Materials Science and Engineering and Laboratory for Research on the Structure of Matter, University of Pennsylvania, Philadelphia, Pennsylvania 19104 and Materials Science and Engineering Laboratory, National Institute of Standards and Technology, Gaithersburg, Maryland 20899

P. A. Heiney
Department of Physics and Laboratory for Research on the Structure of Matter, University of Pennsylvania, Philadelphia, Pennsylvania 19104

P. W. Stephens
Department of Physics, State University of New York, Stony Brook, New York 11794

R. L. Cappelletti
Department of Physics and Astronomy, Ohio University, Athens, Ohio 45701

D. A. Neumann
Materials Science and Engineering Laboratory, National Institute of Standards and Technology, Gaithersburg, Maryland 20899

W. H. Mueller, H. Mohn, and H.-U. ter Meer
Central Research, Hoechst A.G., D-65926 Frankfurt am Main, Germany
(Received 21 October 1993; revised manuscript received 31 January 1994)

Modulated differential scanning calorimetry of sublimed C_{70} shows clear evidence for four first-order transitions, two strong and two weak, which we associate with the two different molecular rotational degrees of freedom in majority (equilibrium) and minority (metastable) phases. The latter correspond to two different stacking sequences of close-packed layers, and their relative contributions to the thermal data correlate well with high-temperature x-ray powder-diffraction results. The upper (long axis tumbling) transition in the majority phase exhibits 50 K supercooling when scanned at 2 K/min. C_{60} impurities at the few % level depress the transition temperatures substantially.

The temperature-dependent molecular dynamics and related structural phase transition in solid C_{60} have been the subject of extensive research.[1–4] Similar work on solid C_{70} has been hampered by difficulties in preparing samples which exhibit intrinsic behavior, and by the existence of metastable phases which cannot be completely eliminated from bulk samples. There are also discrepancies in the literature regarding the critical temperatures for presumably the same phase transitions measured by different groups using different techniques. The purposes of this paper are to resolve some of these discrepancies and to further elucidate the effects of metastable minority phases in near-ideal samples. We also show that relatively small concentrations of C_{60} impurity have a profound effect on the transition temperatures.

The C_{60} molecule is to a good approximation isotropic, and in the solid there is a single thermodynamic transition associated with a crossover from quasifree rotation to a ratcheting or jump rotational diffusion.[3] In contrast, C_{70} possesses a unique axis, from which one expects and observes two transitions corresponding to the sequential freezing out of the tumbling of the long axis and spinning about that axis.[5] These processes have been studied in detail by NMR,[6–8] μSR,[9] and neutron scattering.[10]

For both fullerenes, all of the crystal structures can be described as stacking sequences of close-packed monomolecular layers; the various Bravais lattices observed (monoclinic, rhombohedral, hexagonal, or cubic) are determined by the interlayer stacking and the molecular order (or lack thereof) with respect to the stacking axis. For C_{60} the stacking sequence at all temperatures is unambiguously *ABCABC...*, thus the crystal structures are face-centered cubic (fcc) and simple cubic (sc) in the plastic crystal and orientationally ordered phases, respectively. For C_{70}, both *ABCABC....* and *ABAB....* sequences are observed,[11] and each appears to exhibit its own unique sequence of orientational transitions.[4] This is presumably because second-neighbor interactions

have a non-negligible effect on the temperatures at which both rotational degrees of freedom freeze out. The *ABCABC*.... structures are the equilibrium ones;[12] transitions within this sequence are reversible while sublimation and extended annealing reduces but does not completely eliminate contributions from structures with *ABAB*... stacking. Thus the equilibrium high-T limit is fcc rather than hcp, either of which could accommodate close packing of spherically averaged C_{70} molecules.

X-ray diffraction of highly purified, sublimed, and annealed C_{70} shows that $\sim$ 90% of the molecules are in the fcc structure at high temperature.[5] Orientational disorder evolves in two stages, as manifested by two first-order transitions upon heating: monoclinic $\rightarrow$ rhombohedral at $\sim$ 280 K (onset of uniaxial spinning), and rhombohedral $\rightarrow$ fcc at $\sim$ 330 K d(quasifree tumbling).[5,12] Other groups have reported different temperatures for the same transitions. For example, Christides *et al.*[10] observed the fcc $\rightarrow$ rhombohedral transition below room temperature *on cooling* using neutron diffraction. Meingast *et al.*[13] used high-resolution dilatometry and x-ray diffraction to study single crystal C_{70}; they saw only a single transition at 240 K, interpreted as a transition from the lowest-temperature phase to the fcc phase. Their crystal was not intact after the transition, but was broken into small pieces, presumably because of strains during the transition. Tea *et al.*[14] also observed that the temperature of the (single) thermal conductivity anomaly in C_{70} was strongly dependent on the thermal history and solvent concentration of the sample.

We studied three samples prepared at Hoechst. "Lab grade" sample 1 contained 1.9% C_{60} impurity by high-performance liquid chromatography (HPLC). "Gold grade" sample 2 contained 1.2% C_{60}. Sample 3 was sublimed from "gold grade" at 650 °C in flowing helium at atmospheric pressure; the purest fraction after sublimation showed no detectable C_{60} in HPLC and consisted of well-faceted crystals of typical and maximum dimensions 0.5 mm and 1 mm, respectively. All three samples were studied by standard differential scanning calorimetry (DSC). Sample 3 was also studied by modulated DSC (MDSC), a recently commercialized technique in which a sinusoidally varying heat input is superimposed on the normal linear temperature ramp.[15] The additional variables introduced are the amplitude of the temperature cycle and its period. In this way, the "reversing" and "nonreversing" components of the heat flow can be determined by Fourier transformation, in addition to the total heat flow. Note that the term "reversing" is used rather than "reversible," as this process cannot be strictly in equilibrium under the typical heating and cooling rates used in DSC. It is nontheless possible to determine the specific heat as a function of temperature in a single run provided that the cell has been calibrated.[16]

Figure 1 shows the DSC curves for the three samples. Sample 1 as received showed no endotherms on heating but rather a large one-time exotherm at 330 K, a typical signature of toluene release. After heating to 470 K we reproducibly observed the two broad but distinct endotherms shown in Fig. 1. Samples 2 and 3 gave no evidence of solvent retention; the data shown for these

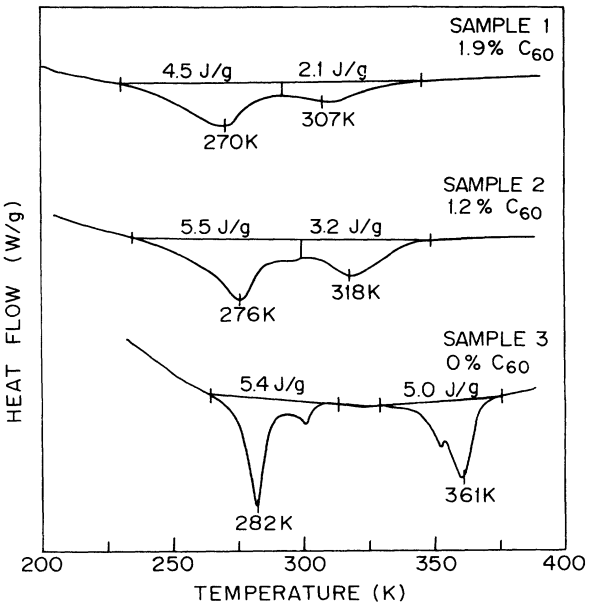

FIG. 1. DSC thermal curves measured on heating, for three samples of C_{70} containing different concentrations of C_{60} impurity as described in the text. Heats of transition obtained by integrating between the indicated limits are included. The *absolute* values are somewhat arbitrary given the nonideal baselines, but the evolution of *relative* heats of the upper and lower transitions with increasing purity is significant.

samples were typical of all cycles including the first. In all samples there appear to be two major transitions, sample 3 showing two additional weaker features. All transitions shift to higher temperatures with increasing purity, the effect being most dramatic for the highest-temperature peak which also increases in amplitude relative to the lower one. The total heat of transition increases from 6.6 to 10.4 J/g from the least to the most pure sample, an effect which has been previously noted in our work on C_{60}. Finally, the transitions become sharper with increasing purity (also typical of C_{60}); only in sample 3 can all four transitions be clearly identified. This progression is consistent with previous work in which the high-temperature transition, with onset above 330 K upon heating, was only observed on sublimed material.[5]

Sample 3 was also examined by MDSC, using an overall 2 K/min heating and cooling rate and a $\pm$1.5 K modulation amplitude with 1/60 Hz frequency. Curves of heat capacity vs temperature are shown in Fig. 2. The two upper pairs of curves (runs 1 and 2) were measured sequentially in a hermetically sealed aluminum cell. The third (run 3) was measured on the same sample which had been removed and placed in a crimped aluminum cell in order to give better thermal contact and also to measure the absolute heat capacity for which this cell had been calibrated. The four transitions observed in DSC are now clearly seen both on heating and cooling. These are labeled 1, 2, 3, and 4 and their primed analogs, for heating and cooling, respectively, and appear to be two coupled sets: 1 and 4 (strong), 2 and 3 (weak). Temperature differences between primed and unprimed peak positions

show that transitions 1 and 2 have very small supercooling (2–3 K) while transitions 3 and 4 show large supercoolings, 15 K and 50 K (peak to peak), respectively. The overall curves are very reproducible although cycling through the upper transition caused some loss of definition, particularly for peak 3. This correlates with the observation that cycling through the high-temperature transition leads to a marked reduction in average crystallite size as shown in Fig. 3.

Figures 1 and 2 are strongly suggestive of coexisting majority and minority phases with *ABCABC*... and *ABAB*... stacking, for which the completely disordered (high-temperature) structures are fcc and hcp, respectively. Figure 4 shows an x-ray powder-diffraction profile obtained at 93 °C from sample 3 after grinding to a fine powder to avoid preferred orientation effects (dots), along with a model fit (solid curve). Most of the reflections can

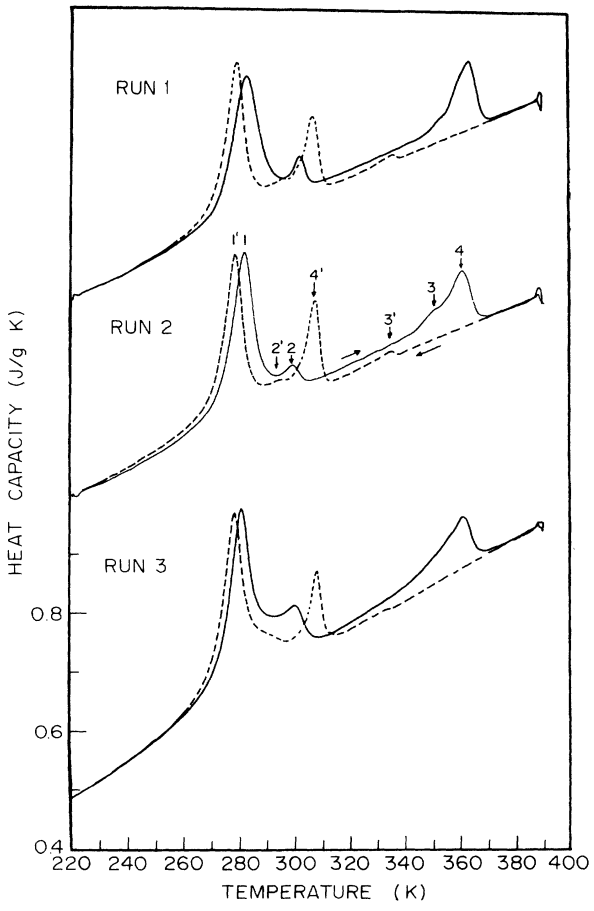

FIG. 2. Heat capacity vs temperature of a ~ 12 mg sublimed C_{70} sample, using MDSC. Solid and dashed curves measured on heating and cooling, respectively. The first two runs were made in a hermetically sealed cell, while run 3 was made after transferring the sample into a calibrated crimped cell. Peaks labeled 1 and 4 are attributed to the two different transitions in the majority phase, while peaks 2 and 3 are associated with a minority phase. Assuming equal molar heats, the minority phase is 14% of the total. Note the marked supercooling effect, ~ 15 K and 50 K, respectively, of peaks 3 and 4.

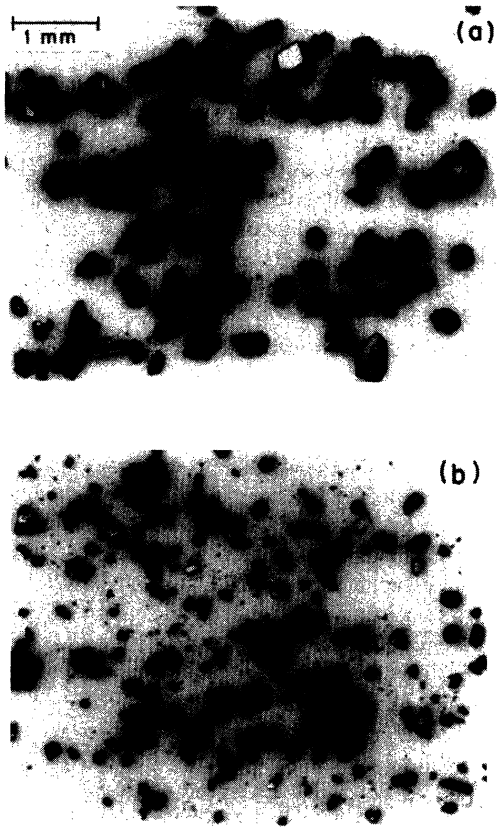

FIG. 3. Photomicrographs of sublimed C_{70} (a) as received, and (b) after heating through the upper transition in the MDSC apparatus. Most of the large crystals have disintegrated into fine powder after temperature cycling.

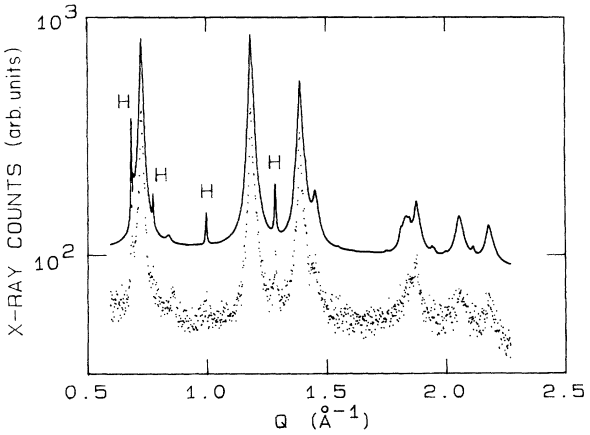

FIG. 4. X-ray powder profile at 93 °C of sublimed and ground C_{70}, measured on beamline X3B1 at the Brookhaven National Synchrotron Light Source (dots). Peaks labeled "*H*" are uniquely indexable as hcp; the others contain hcp and fcc contributions. The solid curve is a two-phase fit from which the hcp mole fraction is 16±6%, consistent with the MDSC. The refined lattice constants are a(fcc) = 14.974 Å, a(hcp) = 10.614 Å, and c = 17.311 Å. Intensities are plotted on a log scale; data and fit have been offset for clarity.

be indexed as either fcc or hcp; the few labeled "*H*" are uniquely indexable as hcp. The overall profile is qualitatively similar to the one presented in Ref. 5 and was analyzed with the identical two-phase model. The grinding process broadens the reflections considerably, more for the fcc component than the hcp one. From a systematic analysis including the matrix of correlations among the fit parameters, we conservatively estimate that 16 ±6% of this sample is hcp. Similarly, the MDSC integrated intensity ratio $I_2/(I_1 + I_2)$ is 14%. Thus (assuming equal *molar* heats for the two phases) the stronger thermal peaks 1 and 4 may be assigned to the majority *ABCABC...* constituent while peaks 2 and 3 involve the same orientational degrees of freedom in the minority *ABAB...* constituent. This implies interesting second-neighbor effects—the spinning transition occurs ~ 20 K higher in the *ABAB...* constituent for both heating and cooling, while the tumbling transition occurs either 10 K lower on heating or 30 K higher on cooling.

We tried a second method to obtain reasonable x-ray powder averaging without broadening the peaks. This consisted of repeatedly "chopping" the sublimed crystals on a glass plate with a razor blade, which indeed resulted in much sharper and stronger peaks as shown in Fig. 5(a) (dots), but the fit (solid curve) revealed a much larger *ABAB...* fraction, 48±20%. Figure 5(b) shows the MDSC of the "chopped" material. Peak 2 is considerably stronger than before (Fig. 2), and the area ratio $I_2/(I_1 + I_2)$ is now 37%. Peak 3 is too broad to resolve, but the long tail on the low-T side of peak 4 suggests considerable intensity in the same T range as before. These results reinforce our conclusion that peaks 2 and 3 are to be associated with transitions in the *ABAB...* sequence. The different fcc/hcp fractions exhibited by the ground and "chopped" sublimed samples probably reflect the macroscopic inhomogeneity of the original batch of large crystals.

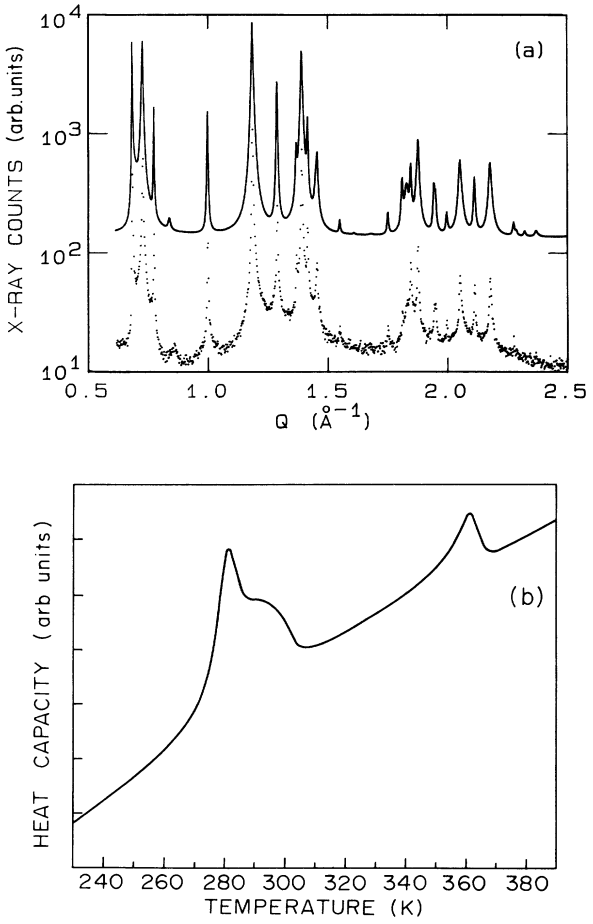

FIG. 5. (a) X-ray powder profile at 108 °C of "chopped" sublimed C_{70} (dots), along with a two-phase fit (solid curve) which gives an hcp mole fraction 48±20%. Refined lattice constants are a(fcc) = 14.980 Å, a(hcp) = 10.606 Å, and c = 17.266 Å. (b) MDSC of the same material (heating curve only), showing an area ratio $I_2/(I_1 + I_2)$ = 37%, consistent with the x-ray analysis of this sample but larger than the MDSC ratio and x-ray analysis of the other sublimed sample.

Transitions 1 and 2 correspond to the onset of rotational motion about the long axis of the C_{70} molecule on heating, while transitions 3 and 4 signal the onset of quasi-isotropic tumbling. The latter motion requires a much larger free volume than the former, which may explain why these transitions exhibit the dramatically larger supercooling. The large temperature difference between peaks 4′ and 4, ~ 50 K, explains why Christides *et al.* observed different neutron diffraction patterns at 300 K approached from lower and higher temperatures. The tumbling transition also provokes the greatest perturbation to the crystal symmetry as well as a ~ 3% change in molar volume,[12] and is most likely the transition responsible for the breakup of the large crystallites shown in Fig. 3. The *total* heat of transition, 10.4 J/g, found for the purest and most perfect C_{70} sample is almost evenly divided between the two transitions, and is similar to that found for the *single* transition in pure C_{60}.

The absolute specific heat of sample 3 is substantially smaller than that found from a rather impure sample;[17] at 220 K (where supercooling is unimportant) we find 0.48 J/gK (Fig. 2) while Grivei *et al.* obtained 1.1 J/g K. The origin of this large discrepancy is not known.

The fcc → rhombohedral transition shifts to higher T with hydrostatic pressure at a rate dT_c/dP = 400 K/GPa near $P = 0$.[18] This suggests that the suppression of T_c by C_{60} impurities, Fig. 1, might be due in part to a negative pressure effect associated with the relaxation of C_{70} neighbors into the free volume around the smaller impurity molecule.[19] We estimate this contribution using the rule of mixtures and the respective fcc lattice constants to obtain the excess volume $\Delta V/V = 0.17x$ where x is the C_{60}/C_{70} impurity fraction, and the relations $P = -B(\Delta V/V)$ and $\Delta T_c = P(dT_c/dP)$ where B is the (rhombohedral) bulk modulus (11 GPa).[18] This results in a suppression of ~ 7 K per % C_{60}. The overall shift of the upper transition in Fig. 1 is much larger, ~ 30 K per %, and the discrepancy is even worse if we consider only the two purest samples. On the other hand, this simple estimate gives a good account of the nearly linear shift of the lower transition, ~ 6 K per %. The C_{70} molar volume decreases by only 3% at both transitions.[12] This is considerably less than the 17% difference between C_{60} and C_{70} molar volumes, so our calculated ΔT_c may be a good

estimate for the monoclinic → rhombohedral transition as well (assuming that B and dT_c/dP are not too different). We conclude that the C_{60} impurity effect on the monoclinic → rhombohedral transition can be qualitatively understood in terms of negative pressure, whereas the rhombohedral → fcc transition is affected by impurities in a more complicated way.

The combined influences of C_{60} impurities and supercooling can easily account for the range of transition temperatures reported for nominally pure C_{70}, so it will be important to specify these quantities in further studies of this interesting system. It would also be of great interest to carry out systematic studies on well-characterized alloys in which all the important secondary variables (crystallite size, solvent retention, intercalated gasses) are carefully controlled.

We are grateful to TA Instruments Inc. for lending us the MDSC apparatus, and to R. M. Strongin, L. Brard, J. Carter, and A. Lommen for experimental assistance. The Penn contribution to this work was supported by the National Science Foundation MRL Program under Grant No. DMR91-20668, and the SUNY X3 beamline is supported by the U. S. Department of Energy under Grant No. DEFG-0291-ER45231.

[1] P. A. Heiney, J. Phys. Chem. Solids **53**, 1333 (1992).
[2] D. A. Neumann, J. R. D. Copley, D. Reznik, W. A. Kamitakahara, J. J. Rush, R. L. Paul, and R. M. Lindstrom, J. Phys. Chem. Solids **54**, 1699 (1993).
[3] J. D. Axe, S. C. Moss, and D. A. Neumann, in *Solid State Physics*, edited by H. Ehrenreich and F. Spaepen (Academic, New York, in press), Vol. 48.
[4] J. E. Fischer and P. A. Heiney, J. Phys. Chem. Solids **54**, 1725 (1993).
[5] G. B. M. Vaughan, P. A. Heiney, J. E. Fischer, D. E. Luzzi, D. A. Ricketts-Foot, A. R. McGhie, Y.-W. Hui, A. L. Smith, D. E. Cox, W. J. Romanow, B. H. Allen, N. Coustel, J. P. McCauley, Jr., and A. B. Smith, III, Science **254**, 1350 (1991).
[6] Y. Maniwa, A. Ohi, K. Mizoguchi, K. Kume, K. Kikuchi, K. Saito, I. Ikemoto, S. Suzuki, and Y. Achiba, J. Phys. Soc. Jpn. **62**, 1131 (1993).
[7] R. Tycko, G. Dabbagh, G. B. M. Vaughan, P. A. Heiney, R. M. Strongin, M. A. Cichy, and A. B. Smith, III, J. Chem. Phys. **99**, 7554 (1993).
[8] R. Blinc, J. Seliger, J. Dolinsek, and D. Arcon (unpublished).
[9] K. Prassides, T. J. S. Dennis, C. Christides, E. Roduner, H. W. Kroto, R. Taylor, and D. R. M. Walton, J. Phys. Chem. **96**, 10600 (1992).
[10] C. Christides, T. J. S. Dennis, K. Prassides, R. L. Cappelletti, D. A Neumann, and J. R. D. Copley, Phys. Rev. B **49**, 2897 (1994).
[11] M. A. Verheijen, H. Meekes, G. Meijer, P. Bennema, J. L. de Boer, S. van Smaalen, G. van Tendeloo, S. Amelinckx, S. Muto, and J. van Landuyt, Chem. Phys. **166**, 287 (1992); G. van Tendeloo, S. Amelinckx, J. L. de Boer, S. van Smaalen, M. A. Verheijen, H. Meekes, and G. Meijer, Europhys. Lett. **21**, 329 (1993).
[12] G. B. M. Vaughan, P. A. Heiney, D. E. Cox, J. E. Fischer, A. R. McGhie, A. L. Smith, R. M. Strongin, M. A. Cichy, and A. B. Smith, III, Chem. Phys. **178**, 599 (1993).
[13] C. Meingast, F. Gugenberger, M. Haluska, H. Kuzmany, and G. Roth, Appl. Phys. A **56**, 227 (1993).
[14] N. H. Tea, R.-C. Yu, M. B. Salamon, D. C. Lorents, R. Malhotra, and R. S. Ruoff, Appl. Phys. A **56**, 219 (1993).
[15] US Patent #5224775 (1993).
[16] DSC 2910 Operator's Manual, Appendix E "Modulated DSC," TA Instruments, Inc., 109 Lukens Drive, Newcastle, DE 19720 (1992).
[17] E. Grivei, B. Nysten, J.-P. Issi, C. Fabre, and A. Rassat, Phys. Rev. B **47**, 1705 (1993).
[18] H. Kawamura, Y. Akahama, M. Kobayashi, H. Shinohara, H. Sato, Y. Saito, T. Kikegawa, O. Shimomura, and K. Aoki, J. Phys. Chem. Solids **54**, 1675 (1993).
[19] We tacitly assume that the large sample-dependent shifts in Fig. 1 are dominated by the varying C_{60} content. Experience with C_{60} suggests that this is reasonable, other contributions (traces of residual solvent, crystallite size, intercalated gasses, etc.) being of order a few K.

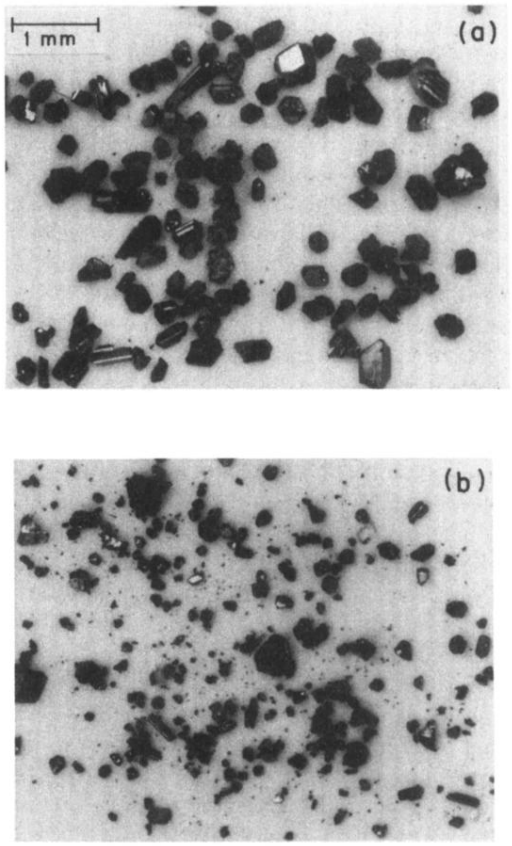

FIG. 3. Photomicrographs of sublimed C_{70} (a) as received, and (b) after heating through the upper transition in the MDSC apparatus. Most of the large crystals have disintegrated into fine powder after temperature cycling.